

AD-A032 087

OAKLAND UNIV ROCHESTER MICH SCHOOL OF ENGINEERING
NEW OPTICAL METHOD TO DETERMINE VIBRATION-INDUCED STRAINS WITH --ETC(U)
NOV 76 Y Y HUNG, J D HOVANESIAN, A J DURELLI N00014-76-C-0487

F/G 20/11

UNCLASSIFIED

41

NL

1 OF 1
ADA032087



AD A 032087

[Handwritten signature]

NEW OPTICAL METHOD TO DETERMINE VIBRATION-INDUCED STRAINS
WITH VARIABLE SENSITIVITY AFTER RECORDING

BY

Y. Y. HUNG, J. D. HOVANESIAN AND A. J. DURELLI

SPONSORED BY

OFFICE OF NAVAL RESEARCH
DEPARTMENT OF THE NAVY
WASHINGTON, D.C. 20025

ON

CONTRACT No. N00014-76-C-0487
O.U. PROJECT No. 38472-86
REPORT No. 41

NATIONAL SCIENCE FOUNDATION
WASHINGTON, D.C. 20550

ON

GRANT No. ENG 76-08751
O.U. PROJECT No. 38510-24

SCHOOL OF ENGINEERING
OAKLAND UNIVERSITY
ROCHESTER, MICHIGAN 48063

[Large handwritten signature]

NOVEMBER 1976

DDC
RECEIVED
NOV 12 1976
B

DISTRIBUTION STATEMENT A
Approved for public release;
Distribution Unlimited

405252

NEW OPTICAL METHOD TO DETERMINE VIBRATION-INDUCED STRAINS
WITH VARIABLE SENSITIVITY AFTER RECORDING

by

Y. Y. Hung, J. D. Hovanesian and A. J. Durelli

Sponsored by

Office of Naval Research
Department of the Navy
Washington, D.C. 20025
on
Contract No. N00014-76-C-0487
O.U. Project No. 38472-86
Report No. 41

National Science Foundation
Washington, D.C. 20550
on
Grant No. ENG 76-08751
O.U. Project No. 38510-24

School of Engineering
Oakland University
Rochester, Michigan 48063

November 1976

ACCESSION for	
NTIS	White Section <input checked="" type="checkbox"/>
DDC	Buff Section <input type="checkbox"/>
UNANNOUNCED	<input type="checkbox"/>
JUSTIFICATION	
BY	
DISTRIBUTION/AVAILABILITY CODES	
Dist.	AVAIL. and/or SPECIAL
A	

NEW OPTICAL METHOD TO DETERMINE VIBRATION-INDUCED STRAINS
WITH VARIABLE SENSITIVITY AFTER RECORDING

by

Y. Y. Hung, J. D. Hovanesian and A. J. Durelli

ABSTRACT

↓ A steady-state vibrating object is illuminated with coherent light and its image is slightly misfocused in the film plane of a camera. The resulting processed film is called a "time-integrated specklegram." When the specklegram is Fourier filtered, it exhibits fringes depicting derivatives of the vibrational amplitude. The direction of the spatial derivative, as well as the fringe sensitivity may be easily and continuously varied during the Fourier filtering process. Besides the above mentioned advantages, this new method is also much less demanding than holographic interferometry with respect to vibration isolation, optical set-up time, illuminating source coherence, required film resolution, etc. ↗

Previous Technical Reports to the Office of Naval Research

1. A. J. Durelli, "Development of Experimental Stress Analysis Methods to Determine Stresses and Strains in Solid Propellant Grains"--June 1962. Developments in the manufacturing of grain-propellant models are reported. Two methods are given: a) cementing routed layers and b) casting.
2. A. J. Durelli and V. J. Parks, "New Method to Determine Restrained Shrinkage Stresses in Propellant Grain Models"--October 1962. The birefringence exhibited in the curing process of a partially restrained polyurethane rubber is used to determine the stress associated with restrained shrinkage in models of solid propellant grains partially bonded to the case.
3. A. J. Durelli, "Recent Advances in the Application of Photoelasticity in the Missile Industry"--October 1962. Two- and three-dimensional photoelastic analysis of grains loaded by pressure and by temperature are presented. Some applications to the optimization of fillet contours and to the redesign of case joints are also included.
4. A. J. Durelli and V. J. Parks, "Experimental Solution of Some Mixed Boundary Value Problems"--April 1964. Means of applying known displacements and known stresses to the boundaries of models used in experimental stress analysis are given. The application of some of these methods to the analysis of stresses in the field of solid propellant grains is illustrated. The presence of the "pinching effect" is discussed.
5. A. J. Durelli, "Brief Review of the State of the Art and Expected Advance in Experimental Stress and Strain Analysis of Solid Propellant Grains"--April 1964. A brief review is made of the state of the experimental stress and strain analysis of solid propellant grains. A discussion of the prospects for the next fifteen years is added.
6. A. J. Durelli, "Experimental Strain and Stress Analysis of Solid Propellant Rocket Motors"--March 1965. A review is made of the experimental methods used to strain-analyze solid propellant rocket motor shells and grains when subjected to different loading conditions. Methods directed at the determination of strains in actual rockets are included.
7. L. Ferrer, V. J. Parks and A. J. Durelli, "An Experimental Method to Analyze Gravitational Stresses in Two-Dimensional Problems"--October 1965. Photoelasticity and moiré methods are used to solve two-dimensional problems in which gravity-stresses are present.

8. A. J. Durelli, V. J. Parks and C. J. del Rio, "Stresses in a Square Slab Bonded on One Face to a Rigid Plate and Shrunk"--November 1965.
A square epoxy slab was bonded to a rigid plate on one of its faces in the process of curing. In the same process the photoelastic effects associated with a state of restrained shrinkage were "frozen-in." Three-dimensional photoelasticity was used in the analysis.
9. A. J. Durelli, V. J. Parks and C. J. del Rio, "Experimental Determination of Stresses and Displacements in Thick-Wall Cylinders of Complicated Shape"--April 1966.
Photoelasticity and moiré are used to analyze a three-dimensional rocket shape with a star shaped core subjected to internal pressure.
10. V. J. Parks, A. J. Durelli and L. Ferrer, "Gravitational Stresses Determined Using Immersion Techniques"--July 1966.
The methods presented in Technical Report No. 7 above are extended to three-dimensions. Immersion is used to increase response.
11. A. J. Durelli and V. J. Parks. "Experimental Stress Analysis of Loaded Boundaries in Two-Dimensional Second Boundary Value Problems"--February 1967.
The pinching effect that occurs in two-dimensional bonding problems, noted in Reports 2 and 4 above, is analyzed in some detail.
12. A. J. Durelli, V. J. Parks, H. C. Feng and F. Chiang, "Strains and Stresses in Matrices with Inserts,"-- May 1967.
Stresses and strains along the interfaces, and near the fiber ends, for different fiber end configurations, are studied in detail.
13. A. J. Durelli, V. J. Parks and S. Uribe, "Optimization of a Slot End Configuration in a Finite Plate Subjected to Uniformly Distributed Load,"--June 1967.
Two-dimensional photoelasticity was used to study various elliptical ends to a slot, and determine which would give the lowest stress concentration for a load normal to the slot length.
14. A. J. Durelli, V. J. Parks and Han-Chow Lee, "Stresses in a Split Cylinder Bonded to a Case and Subjected to Restrained Shrinkage,"--January 1968.
A three-dimensional photoelastic study that describes a method and shows results for the stresses on the free boundaries and at the bonded interface of a solid propellant rocket.
15. A. J. Durelli, "Experimental Stress Analysis Activities in Selected European Laboratories"--August 1968.
This report has been written following a trip conducted by the author through several European countries. A list is given of many of the laboratories doing important experimental stress analysis work and of the people interested in this kind of work. An attempt has been made to abstract the main characteristics of the methods used in some of the countries visited.

16. V. J. Parks, A. J. Durelli and L. Ferrer, "Constant Acceleration Stresses in a Composite Body"--October 1968.
Use of the immersion analogy to determine gravitational stresses in two-dimensional bodies made of materials with different properties.
17. A. J. Durelli, J. A. Clark and A. Kochev, "Experimental Analysis of High Frequency Stress Waves in a Ring"--October 1968.
A method for the complete experimental determination of dynamic stress distributions in a ring is demonstrated. Photoelastic data is supplemented by measurements with a capacitance gage used as a dynamic lateral extensometer.
18. J. A. Clark and A. J. Durelli, "A Modified Method of Holographic Interferometry for Static and Dynamic Photoelasticity"--April 1968.
A simplified absolute retardation approach to photoelastic analysis is described. Dynamic isopachics are presented.
19. J. A. Clark and A. J. Durelli, "Photoelastic Analysis of Flexural Waves in a Bar"--May 1969.
A complete direct, full-field optical determination of dynamic stress distribution is illustrated. The method is applied to the study of flexural waves propagating in a urethane rubber bar. Results are compared with approximate theories of flexural waves.
20. J. A. Clark and A. J. Durelli, "Optical Analysis of Vibrations in Continuous Media"--June 1969.
Optical methods of vibration analysis are described which are independent of assumptions associated with theories of wave propagation. Methods are illustrated with studies of transverse waves in prestressed bars, snap loading of bars and motion of a fluid surrounding a vibrating bar.
21. V. J. Parks, A. J. Durelli, K. Chandrashekhara and T. L. Chen, "Stress Distribution Around a Circular Bar, with Flat and Spherical Ends, Embedded in a Matrix in a Triaxial Stress Field"--July 1969.
A Three-dimensional photoelastic method to determine stresses in composite materials is applied to this basic shape. The analyses of models with different loads are combined to obtain stresses for the triaxial cases.
22. A. J. Durelli, V. J. Parks and L. Ferrer, "Stresses in Solid and Hollow Spheres Subjected to Gravity or to Normal Surface Traction"--October 1969.
The method described in Report No. 10 above is applied to two specific problems. An approach is suggested to extend the solutions to a class of surface traction problems.
23. J. A. Clark and A. J. Durelli, "Separation of Additive and Subtractive Moiré Patterns"--December 1969.
A spatial filtering technique for adding and subtracting images of several gratings is described and employed to determine the whole field of Cartesian shears and rigid rotations.

24. R. J. Sanford and A. J. Durelli, "Interpretation of Fringes in Stress-Holo-Interferometry"--July 1970.
Errors associated with interpreting stress-holo-interferometry patterns as the superposition of isopachics (with half order fringe shifts) and isochromatics are analyzed theoretically and illustrated with computer generated holographic interference patterns.
25. J. A. Clark, A. J. Durelli and P. A. Laura, "On the Effect of Initial Stress on the Propagation of Flexural Waves in Elastic Rectangular Bars"--December 1970.
Experimental analysis of the propagation of flexural waves in prismatic, elastic bars with and without prestressing. The effects of prestressing by axial tension, axial compression and pure bending are illustrated.
26. A. J. Durelli and J. A. Clark, "Experimental Analysis of Stresses in a Buoy-Cable System Using a Birefringent Fluid"--February 1971.
An extension of the method of photoviscous analysis is presented which permits quantitative studies of strains associated with steady state vibrations of immersed structures. The method is applied in an investigation of one form of behavior of buoy-cable systems loaded by the action of surface waves.
27. A. J. Durelli and T. L. Chen, "Displacements and Finite-Strain Fields in a Sphere Subjected to Large Deformations"--February 1972.
Displacements and strains (ranging from 0.001 to 0.50) are determined in a polyurethane sphere subjected to several levels of diametral compression. A 500 lines-per-inch grating was embedded in a meridian plane of the sphere and moiré effect produced with a non-deformed master. The maximum applied vertical displacement reduced the diameter of the sphere by 27 per cent.
28. A. J. Durelli and S. Machida, "Stresses and Strain in a Disk with Variable Modulus of Elasticity"--March 1972.
A transparent material with variable modulus of elasticity has been manufactured that exhibits good photoelastic properties and can also be strain analyzed by moiré. The results obtained suggests that the stress distribution in the homogeneous disk. It also indicates that the strain fields in both cases are very different, but that it is possible, approximately, to obtain the stress field from the strain field using the value of E at every point, and Hooke's law.
29. A. J. Durelli and J. Buitrago, "State of Stress and Strain in A Rectangular Belt Pulled Over a Cylindrical Pulley"--June 1972.
Two- and three-dimensional photoelasticity as well as electrical strain gages, dial gages and micrometers are used to determine the stress distribution in a belt-pulley system. Contact and tangential stress for various contact angles and friction coefficients are given.

30. T. L. Chen and A. J. Durelli, "Stress Field in a Sphere Subjected to Large Deformations"--June 1972.
Strain fields obtained in a sphere subjected to large diametral compressions from a previous paper were converted into stress fields using two approaches. First, the concept of strain-energy function for an isotropic elastic body was used. Then the stress field was determined with the Hookean type natural stress-natural strain relation. The results so obtained were also compared.
31. A. J. Durelli, V. J. Parks and H. M. Hasseem, "Helices Under Load"--July 1973.
Previous solutions for the case of close coiled helical springs and for helices made of thin bars are extended. The complete solution is presented in graphs for the use of designers. The theoretical development is correlated with experiments.
32. T. L. Chen and A. J. Durelli, "Displacements and Finite Strain Fields in a Hollow Sphere Subjected to Large Elastic Deformations"--September 1973.
The same methods described in No. 27, were applied to a hollow sphere with an inner diameter one half the outer diameter. The hollow sphere was loaded up to a strain of 30 per cent on the meridian plane and a reduction of the diameter by 20 per cent.
33. A. J. Durelli, H. H. Hasseem and V. J. Parks, "New Experimental Method in Three-Dimensional Elastostatics"--December 1973.
A new material is reported which is unique among three-dimensional stress-freezing materials, in that, in its heated (or rubbery) state it has a Poisson's ratio which is appreciably lower than 0.5. For a loaded model, made of this material, the unique property allows the direct determination of stresses from strain measurements taken at interior points in the model.
34. J. Wolak and V. J. Parks, "Evaluation of Large Strains in Industrial Applications"--April 1974.
It was shown that Mohr's circle permits the transformation of strain from one axis of reference to another, irrespective of the magnitude of the strain, and leads to the evaluation of the principal strain components from the measurement of direct strain in three directions.
35. A. J. Durelli, "Experimental Stress Analysis Activities in Selected European Laboratories"--April 1975.
Continuation of Report No. 15 after a visit to Belgium, Holland, Germany, France, Turkey, England and Scotland.
36. A. J. Durelli, V. J. Parks and J. O. Bühler-Vidal, "Linear and Non-linear Elastic and Plastic Strains in a Plate with a Big Hole Loaded Axially in its Plane"--July 1975.
Strain analysis of the ligament of a plate with a big hole indicates that both geometric and material non-linearity may take place. The strain concentration factor was found to vary from 1 to 2 depending on the level of deformation.

37. A. J. Durelli, V. Pavlin, J. O. Bühler-Vidal and G. Ome, "Elastostatics of a Cubic Box Subjected to Concentrated Loads"--August 1975.
Analysis of experimental strain, stress and deflection of a cubic box subjected to concentrated loads applied at the center of two opposite faces. The ratio between the inside span and the wall thickness was varied between approximately 5 and 121.

38. A. J. Durelli, V. J. Parks and J. O. Bühler-Vidal, "Elastostatics of Cubic Boxes Subjected to Pressure"--March 1976.
Experimental analysis of strain, stress and deflections in a cubic box subjected to either internal or external pressure. Inside span-to-wall thickness ratio varied from 5 to 14.

Introduction

The advantages common to all optical methods in experimental studies of vibrations are that they are noncontacting and generally full-field. These optical methods may be grouped into three categories - moiré methods, holographic interferometric methods, and laser speckle techniques.

A brief review of the moiré methods in visualization of nodes and antinodes in vibrating plate can be found in reference ⁽¹⁾. A projected ruling method ^(2,3) was also developed for studying vibrational amplitudes. A time-dependent perturbed ruling is observed when the ruling is projected onto a vibrating object. Photographing the perturbed ruling with an exposure time of several vibrational periods yields a time-integrated moiré fringes depicting nodal amplitude of the steady state vibration. These fringes can also be seen by eye in real-time if the vibrational frequency is approximately 20 Hz or more. All the moiré methods, however, are limited to studies of vibrations with relatively large amplitudes.

Powell and Stetson ⁽⁴⁾ and other investigators ^(5,6,7) have demonstrated that time-averaged holography is well suitable for analysis of steady-state vibrations with very small amplitudes. In the reconstruction of the hologram which recorded a steady-state vibrating object, a time-averaged fringe pattern is observed which is described by a zero-order Bessel function containing the vibrational amplitude in its argument. Nodal areas are also clearly indicated by the regions of the brightest reconstruction. An extension of this technique, the modulated holography ^(8,9), can be used to

reduce the sensitivity, and to determine the relative phase. Shortcomings of these techniques, however, are those associated with holographic interferometry, such as stringent requirement on mechanical and thermal stabilities, the fringe localization problem, etc.

The speckle pattern produced by the random scattering of a diffused object when illuminated by coherent light acts as an information carrier about the object surface. By simply watching the speckle pattern on a surface while it is undergoing steady state oscillation, one can observe nodal patterns in real time^(10,11,12). This provides a quick and simple way of scanning for the appropriate frequencies to be studied in greater detail. Butters and Leendertz⁽¹³⁾ demonstrated that a time-averaged speckled fringe pattern depicting vibrational amplitudes similar to that of time-averaged holography could be obtained. The sensitivity of their technique is about the same order as that of holography. Nevertheless, it is less demanding on film resolution and speckle fringes localize on the object surface. Another virtue of speckle interferometry over holographic interferometry is that it permits in-plane displacements to be measured independently^(14,15,16). This advantage is particularly useful for in-plane vibration analysis^(17,18).

Another interesting technique for vibration studies is the speckle-shearing interferometer introduced by Hung and Taylor⁽¹⁹⁾. The technique measures derivatives of vibrational amplitudes directly; thus it greatly facilitates the analysis of stresses resulting from vibrations. An improved version was reported by Hung, Rowlands and Daniel⁽²⁰⁾. In their method, the object under study was illuminated by a beam of coherent light and was imaged by a camera having a mask with four apertures in front of the lens. A photographic plate was exposed in the misfocused image plane while the object was undergoing steady-state vibration. The purpose of misfocusing

was to produce a shearing effect. The processed plate was Fourier filtered to yield four families of fringes, each depicting the derivatives of the vibrational amplitudes with respect to the direction parallel to the line joining the centers of each aperture pair. The sensitivity of the method was mainly controlled by the amount of shearing. However, both the derivative directions as well as the sensitivity were fixed after recording.

The present paper describes a new optical technique whereby the derivatives of vibrational amplitudes with respect to all directions can be recorded at one time. Moreover, the sensitivity can be varied after recording.

The fact the technique measures derivatives of vibrational amplitudes is particularly useful for studying flexural stresses induced by vibrations. Since strains due to vibrational bending are proportional to the second derivatives of the amplitudes, it therefore only requires one differentiation to obtain strains as in contrast to those amplitude measuring techniques which need to differentiate the data twice.

The examples presented in Fig. 4 were prepared at low levels of sensitivity in order to show the principle of this technique. For actual quantitative studies, the systems should be adjusted to yield higher fringe densities in order to facilitate accurate determination of the second derivatives.

Description of the Method

Figure 1 illustrates the schematic diagram for recording. The object under study is illuminated by a collimated beam of coherent light inclined at an angle θ to the viewing direction. It is imaged by a camera with the

aperture fully opened. A photographic plate is placed at a small distance S from the image plane. While the object is undergoing steady state oscillations, the photographic plate is exposed with an exposure time equal to many vibrational periods. The processed photographic plate is referred to as a "time integrated specklegram." It will be shown in the following that a fringe pattern contouring the derivatives of the vibrational amplitudes with respect to any desired direction can be extracted from the specklegram with variable sensitivity by a Fourier filtering technique.

Analysis of Recording Process

The full aperture of the lens can be considered as an infinitely dense collection of small aperture pairs. Let us focus on the function of one aperture pair. Let the line joining the centers of the aperture pair be parallel to the r -direction as shown in Figure 2. and d be their separation. The two images of the structure, one focused by each aperture, are coincident in the image plane. Due to the film plane being misfocused, these two images are sheared laterally in the r -direction. The amount of the shearing $\delta r'$ in the film plane is

$$\delta r' = \frac{S}{D_i} d \quad (1)$$

where D_i is the distance of the image plane from the lens, and S is the misfocus. The equivalent shearing δr in the object plane is

$$\delta r \approx \frac{\delta r'}{m} = \frac{S}{m D_i} d \quad (2)$$

where m is the magnification.

Obviously this arrangement brings the ray scattered from a point $P(x,y)$ to meet the ray scattered from a neighboring point $P(x+\delta x, y+\delta y)$ in the film

plane where $\delta x = \delta r \cos\phi$, and $\delta y = \delta r \sin\phi$. If the two apertures are small, they can be considered as a two-point source, and the resulting interference is a ruling whose lines are perpendicular to the r-direction. The frequency f' of the ruling is given by (15,16):

$$f' = \frac{d}{\lambda(D_i + S)} \quad (3)$$

where λ = wavelength of the laser light.

Hence the equivalent frequency f in the object is:

$$f = \frac{dm}{\lambda(D_i + S)} \quad (4)$$

$$= \frac{m^2 D_i}{\lambda S (D_i + S)} \delta \bar{r}$$

The ruling is distorted by the randomness of the speckle pattern. It can be shown that the intensity distribution $I(x,y)$ of the speckle ruling is represented by (19,20).

$$I(x,y) = a^2 [1 + \cos(2\pi fr + \chi)]^* \quad (5)$$

where χ - random speckle phase

a - light amplitude

$x = r \cos\phi; y = r \sin\phi$

It has been assumed in the above analysis that the object is in its stationary position. Suppose that the object is undergoing steady state sinusoidal vibration with a displacement only in the z-direction represented by:

$$W(x,y,t) = A(x,y) \cos(\omega t + \alpha) \quad (6)$$

*For simplicity, the magnification is assumed to be unity and so the image plane would take the same coordinates as the object plane except it is inverted. This assumption is carried on hereafter.

where

$W(x,y,t)$ is the displacement in the z-direction

$A(x,y)$ - amplitude function

ω - circular frequency

α - arbitrary phase

The relative displacement $\delta W(t)$ between the point $P(x,y)$ and the neighboring point $P(x+\delta x, y+\delta y)$ is thus:

$$\delta W(x,y,t) = W(x+\delta x, y+\delta y, t) - W(x,y,t) \quad (7)$$

This relative displacement will cause a relative optical path change and hence the phase between the light scattered from the two points. With the assumption that the object size is small compared to D_0 , this relative phase Δ change can be shown to be approximately given by:

$$\Delta = \frac{2\pi}{\lambda} (1 + \cos\theta) \cdot \delta W(x,y,t) \quad (8)$$

which results in a local optical shift of the speckle-ruling.⁴ Thus equation (5) in which $I(x,y)$ is now time dependent becomes:

$$I(x,y,t) = a^2 [1 + \cos(2\pi fr + \chi + \Delta)] \quad (9)$$

The exposure $E(x,y)$ on the film for a number of vibrational period is therefore an integration of the intensity over the exposure time T given by:

$$E(x,y) = k \int_0^T I(x,y,t) dt \quad (10)$$

where k is the photographic film constant

The above integration yields:

$$E(x,y) = kTa^2 \{1 + \cos(2\pi fr + \chi) \cdot J_0[\beta]\} \quad (11)$$

where

$$\beta = \frac{2\pi}{\lambda} (1 + \cos\theta) [A(x+\delta x, y+\delta y) - A(x,y)] \quad (12)$$

Equation (11) represents a carrier of approximately constant frequency modulated by $J_0[\beta]$, a Bessel function of zero-order. Nulling of the carrier

which will be identified as moire fringes occurs when β equals to the null roots of the zero-order Bessel function. Equation (12) may be rewritten as:

$$\begin{aligned}\beta &= \frac{2\pi}{\lambda}(1 + \cos\theta) \delta r \left[\frac{A(x+\delta x, y+\delta y) - A(x, y)}{\delta r} \right] \\ &= \frac{2\pi}{\lambda}(1 + \cos\theta) \delta r \left[\frac{\delta A(x, y)}{\delta r} \right]\end{aligned}\quad (13)$$

If δr , the lateral shear is small, $\left(\frac{\delta A}{\delta r}\right)$ approaches $\left(\frac{\partial A}{\partial r}\right)$. Hence the fringe pattern depicted by equation (11) is a contour map of the derivatives of the vibrational amplitudes with respect to the r-direction.

It is seen in equation (13) that δr , the amount of shearing, is a sensitivity factor, and it depends upon d , the separation of the aperture centers. Also δr is related to the frequency of ruling by equation (4). Thus an aperture-pair with greater separation produces a greater shearing and hence greater carrier frequency. The direction of the shearing is parallel to the line joining the aperture-pair centers i.e., it is perpendicular to the lines of the ruling. With the orientation of the aperture-pair varied, both the shearing direction and the ruling orientation are changed accordingly.

We have just shown that an aperture-pair is indeed an interferometer measuring the derivatives of the vibrational amplitudes with respect to a direction parallel to the line joining the aperture-pair centers and with sensitivity depending upon the aperture separation. This information is represented by a family of fringes formed by moiré phenomenon of two slightly mismatched speckle-rulings interpreted by equation (11). Since the whole lens aperture consists of many aperture pairs with aperture separation varying from 0 to R , the diameter of the lens, and with the orientation varying from $\phi = 0$ to $\phi = 360^\circ$, recorded on the specklegram are rulings of all orientations and of frequency varying from 0 to $R/\lambda(D_1+S)$. Each ruling forms a fringe family of its own. Therefore a

specklegram contains a superposition of a multiplicity of moiré fringe families. Each fringe family depicts vibrational amplitudes with respect to a direction perpendicular to the ruling-line and with sensitivity depends on the ruling frequency. Thus the derivatives of the vibrational amplitudes with respect to all directions are recorded in the specklegram with a variable range of sensitivity after recording the upper limit depending on the highest frequency which the recording lens is capable of passing.

Readout Process by Fourier Filtering

To readout the fringe family depicting amplitude-derivative with respect to a particular direction and with a desired sensitivity, a readout device shown in Figure 3 is employed. A beam from a laser is expanded by a microscopic objective and is spatially filtered by the pinhole. The beam diverged from the pin hole is focused by a lens to a point lying in a plane known as the Fourier filtering plane. The time-integrated specklegram is placed in the input plane as shown and is imaged by a camera behind the Fourier filtering plane. It will be shown that by inserting a small aperture off-center in the η -direction, a fringe pattern depicting the vibrational amplitude derivative with respect to the η -direction is displayed in the image plane of the camera (output plane) with a sensitivity proportional to the distance of the aperture from the optical center.

It can be shown that what appears in the Fourier filtering plane of Figure 3 is the Fourier transform of the amplitude transmittance of the specklegram multiplied by a quadratic phase term.⁽²¹⁾ This represents a transformation from a spatial domain to a frequency domain. In other words, rulings of different frequency are separated in the Fourier filtering plane. If a small aperture is located at a distance q from the optical axis in

the η -direction, a ruling orthogonal to the η -direction and of frequency f is given by

$$f = \frac{q}{\lambda'Z} \quad (13)$$

where λ = wavelength of light used for filtering is passed. As analyzed above this ruling corresponds to a shearing δr in the η -direction given by:

$$\delta r = \frac{q}{\lambda'Z} \frac{\lambda S(D_i + S)}{D_i} \quad (14)$$

However, areas corresponding to the nulling of the carrier as described in equation (11) makes no contribution. Thus those areas will appear dark in the output plane. Therefore a fringe pattern is observed on the image that depicts the amplitude-derivative with respect to the η -direction accompanied by a sensitivity factor of δr given in equation (15). By varying the η -direction, any desired derivative direction can be chosen with an adjustable sensitivity depending on the distance q .

Experiments

A rectangular plate of dimensions 3.75 x 5.0 cm clamped along its boundaries was chosen for demonstration. The plate was driven by an audio speaker so that it was vibrating at its fundamental frequency. The set up shown in Figure 1 was used for recording whereby a spectra physics 125 laser was used for the illuminating source. The processed time-integrated specklegram was Fourier filtered with the scheme of Figure 3. The specklegrams were recorded on Agfa 10E75 film, typically using exposure times of 1-5 seconds. Photographic processing included 5 minutes in Kodak D-19, 1 minute stop, 5 minutes Fix and 10 minutes wash. Figure 4 shows the fringe patterns extracted from the specklegram depicting the derivatives of the vibrational amplitudes with respect to the various directions as shown, and with different sensitivities.

Summary and Conclusion

A new optical technique has been described which permits derivatives of vibrational amplitudes to be measured directly. One outstanding feature of the technique is that it provides variability after recording, both in derivative direction as well as sensitivity. The method can be viewed as a holographic interferometric method in which every point on the object acts as a reference for all its neighboring points. However, several limitations associated with holography have been alleviated. These include: (1) simple experimental set up; (2) less demanding on stabilities, (3) relaxation of film resolution requirement and (4) providing greater range of sensitivity. A shortcoming of the technique is that fringe visibility is generally poor.

It should be noted that the mechanical shift of speckle-rulings due to lateral displacement (displacement orthogonal to line of sight) is assumed negligible. Should the lateral displacement be appreciable, the mechanical shift must be considered. The combined effect of the optical and mechanical shift of speckle-rulings will be analyzed in a future paper.

Acknowledgment

This research program from which this paper was developed was supported partially by the National Science Foundation (Grant ENG 76-08751), and the Office of Naval Research (Contract No. N-00014-76-C-0487). The authors are grateful to Dr. C. C. Astill of NSF and Dr. N. Perrone of ONR for their encouragement.

The authors also wish to acknowledge that a similar technique is currently being developed independently by Professor F. P. Chiang of the State University of New York at Stony Brook.

References:

1. Hazell, C. R. and Niven, R. D., "Visualization of Nodes and Antinodes in Vibrating Plates," Experimental Mechanics, 225-231, May 1968.
2. Hovanesian, J. D. and Hung, Y. Y., "Moiré Contour-Sum Contour-Difference, and Vibration Analysis of Arbitrary Objects," Applied Optics, Vol. 10, No. 12, 1971.
3. Vest, C. M. and Sweeney, D. W., "Measurement of Vibrational Amplitude by Modulation of Projected Fringes," Applied Optics, Vol. 11, No. 2, 449, 1972.
4. Powell, R. L. and Stetson, K. A., "Interferometric Vibration Analysis by Wavefront Reconstruction," J. Opt. Soc. Am., 55, 1593, 1965.
5. Aleksoff, C. C., "Time Average Holography Extended," Applied Physics Letters, Vol. 14, No. 1, 23, 1969.
6. Neuman, D. B., Jacobson, C. F., and Brown, G. M., "Holographic Technique for Determining the Phase of Vibrating Objects," Applied Optics, Vol. 9, No. 6, 1357, 1970.
7. Monahan, M. A. and Bromley, K., "Vibration Analysis by Holographic Interferometry," J. Aconst. Soc. Am, 44, 1225, 1968.
8. Archbold E. and Ennos, A. C., "Observation of Surface Vibration Modes by Stroboscopic Hologram Interferometry," Nature, 217, 942, 1968.
9. Aleksoff, C. C. "Temporally Modulated Holography," Applied Optics, Vol. 10, No. 6, 1329, 1971.
10. Archbold, E., Burch, J. M., Ennos, A. E. and Taylor, P. A., "Visual Observation of Surface Vibration Nodal Patterns," Nature, Vol. 222, No. 5190, 263-265, 1969.
11. Fernelius, N. and Tome, C., "Vibration-Analysis Studies Using Changes of Laser Speckle," J. Of Opt. Soc. Am. Vol. 61, No. 5, 566-572, 1971.
12. Eliasson, B. and Mottier, F. M., "Determination of the Granular Radiance Distribution of a Diffuser and its Use for Vibration Analysis," J. Opt. Soc. Am., Vol. 61, No. 5, 559-565, 1971.
13. Butters, J. N. and Leendertz, J. A., "Application of Video Techniques and Speckle Pattern Interferometry to Engineering Measurement," Proceedings of the Symposium--Engineering Applications of Holography, Feb. 16-17, 345-360, 1972.
14. Archbold, E., Burch, J. M. and Ennos, A. Z., "Recording of In-plane Surface Displacement by Double Exposure Speckle Photography," Optica Acta, Vol. 17, No. 12, 883-898, 1970.

15. Duffy, D., "Moiré Gauging of In-plane Displacement Using Double Aperture Imaging", Applied Optics, 1778-1781, 1972; also, Experimental Mechanics, September 1974.
16. Hung, Y. Y., Hu, C. P., and Taylor, C. E., "Speckle-Moiré Interferometry - A Tool for Complete Measurement of In-Plane Surface Displacements", Proceedings of 7th Southeastern Conference on Theoretical and Applied Mechanics, 497-505, 1974.
17. Tiziani, H. J., "Application of Speckling for In-Plane Vibration Analysis", Optica Acta, 18, 1971.
18. Archbold, E. and Ennos, A. E., "Two-dimensional Vibrational Analysis by Speckle Photography", Optics and Laser Technology, Feb. 1975.
19. Hung, Y. Y., Rowlands, R. E., and Daniel, I.M., "Speckle-Shearing Interferometric Technique: A Full-Field Strain Gauge", Applied Optics, Vol. 14, No. 3, 618-622, 1975.
20. Hung, Y. Y., and Taylor, C. E., "Speckle-Shearing Interferometric Camera-A Tool for Measurement of Derivatives of Surface Displacements", Proceedings of the Society of Photo-optical Instrumentation Engineers, Vol. 41, 169-175, 1973.
21. Burch, J. M. and Tokarski, J. M. J., "Production of Multiple Beam Fringes from Photographic Scatterers", Optica Acta, Vol. 15, No. 2, 101-111, 1968.

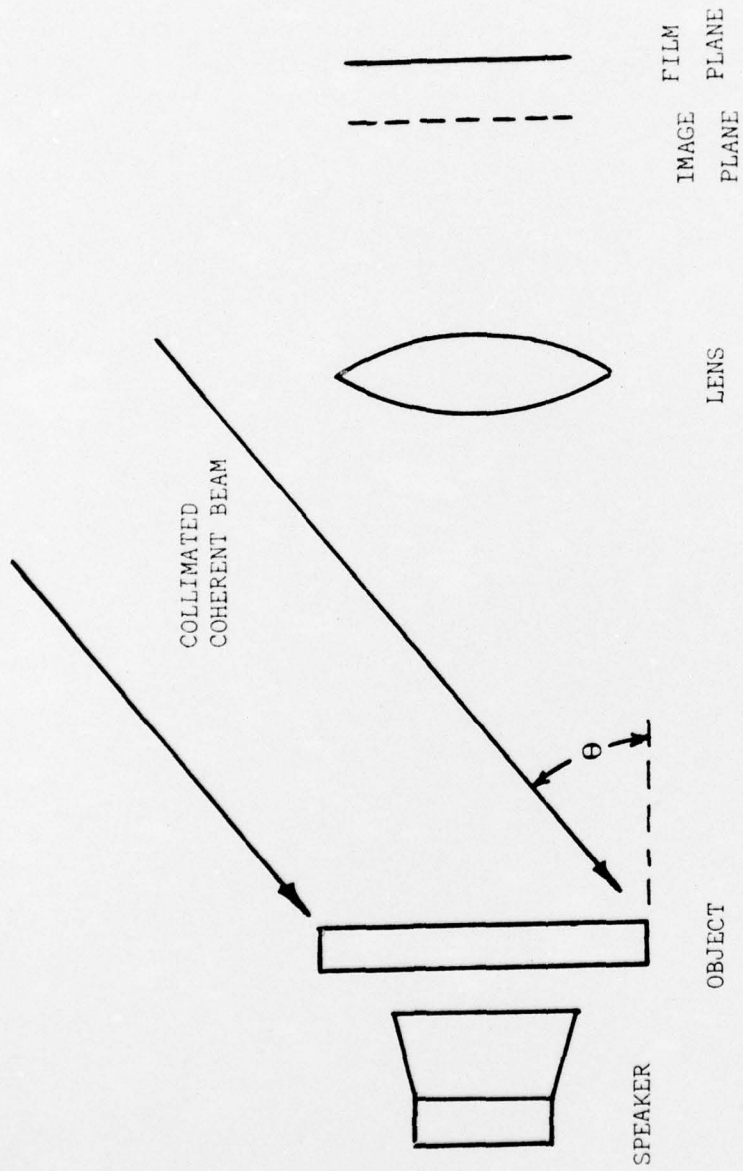
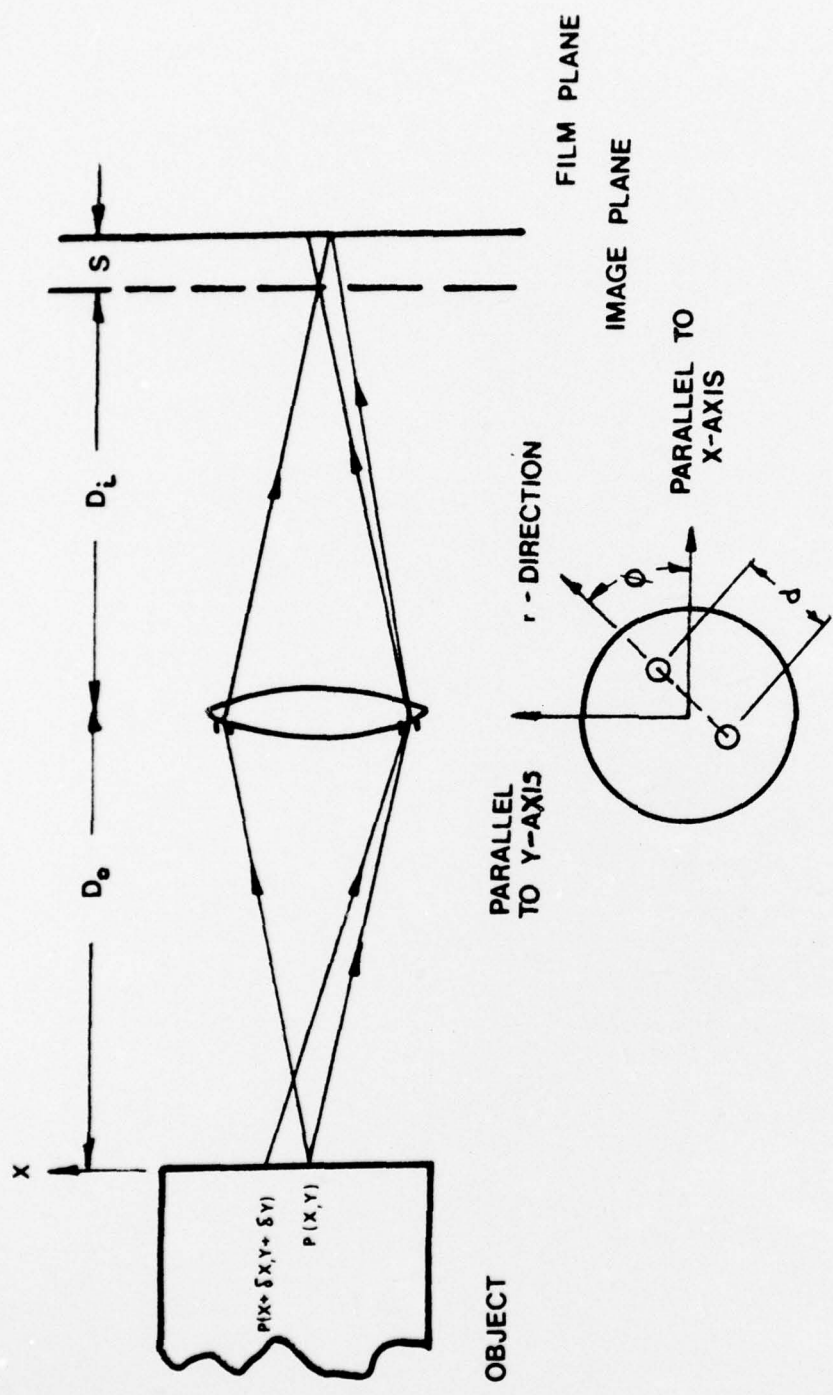
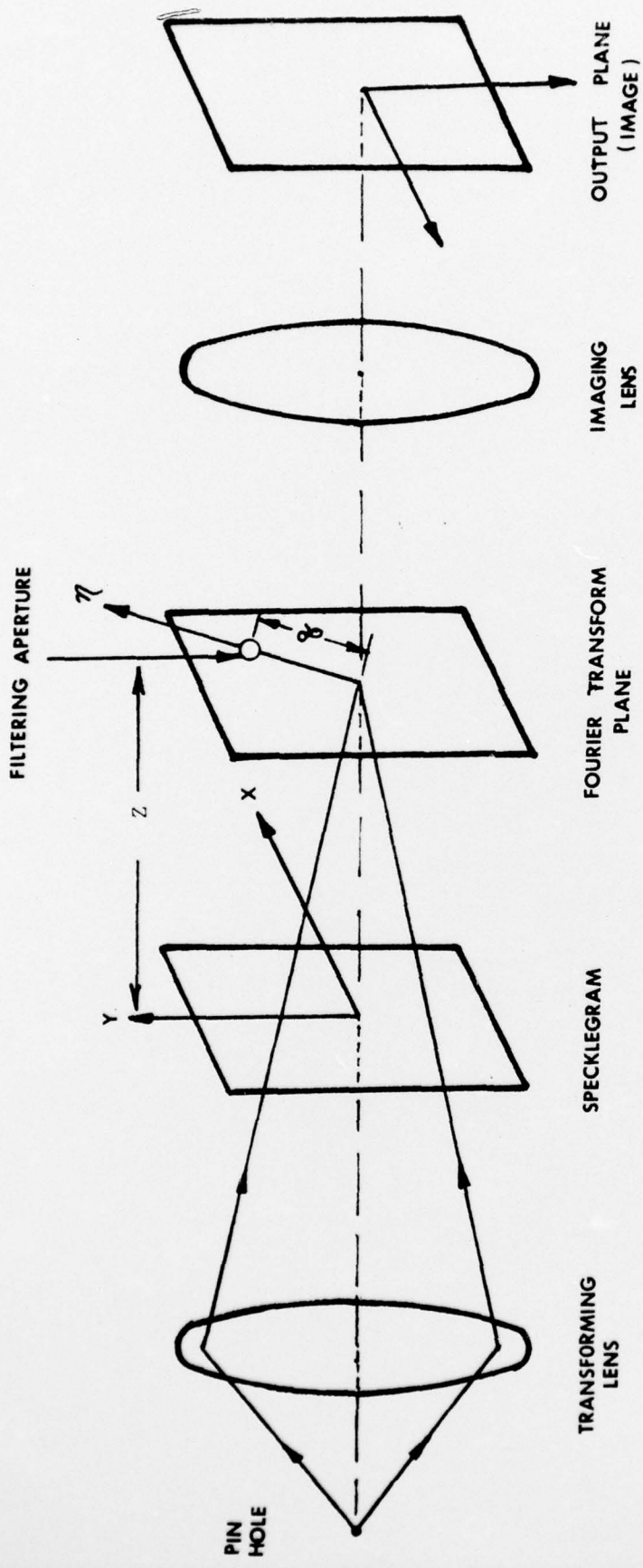


FIGURE 1: SCHEMATIC DIAGRAM FOR RECORDING



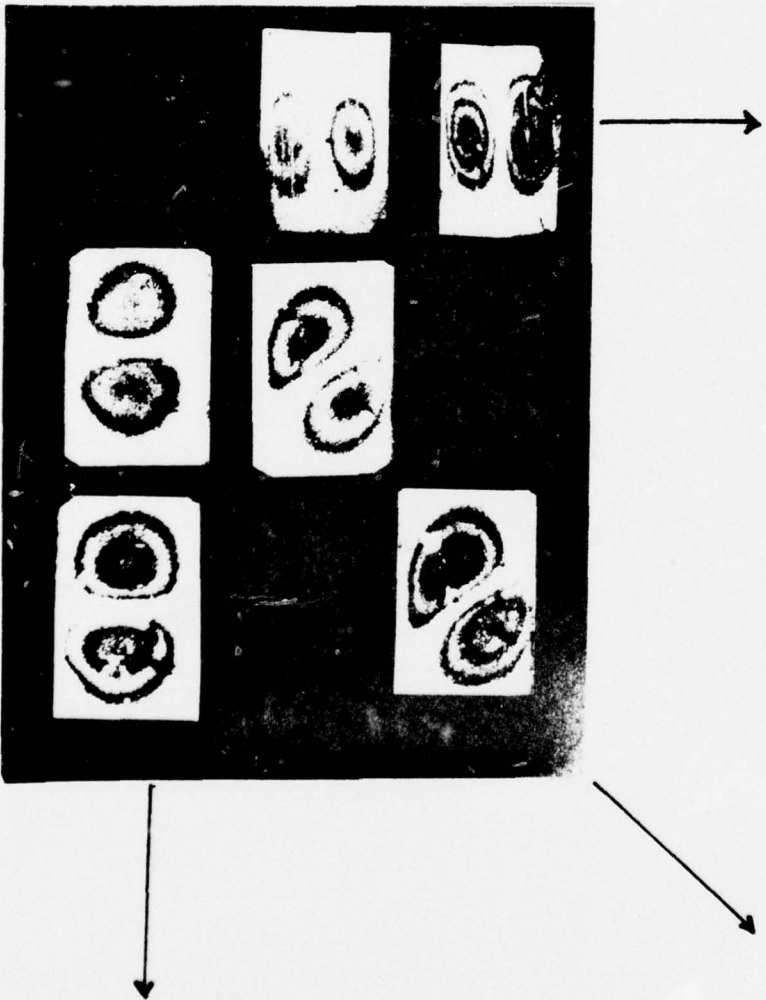
0-16

FIGURE 2 : FUNCTION OF AN APERTURE-PAIR



0-17 1

FIGURE 3: FOURIER FILTERING SCHEME FOR EXTRACTING DISPLACEMENT-DERIVATIVE FRINGES



0-14

FIGURE 4: FRINGE PATTERNS DEPICTING DERIVATIVES OF VIBRATIONAL AMPLITUDES OF THE RECTANGULAR PLATE, PHOTOGRAPHED FROM THE VARIOUS POSITIONS IN THE FILTERING PLANE

ONR DISTRIBUTION LIST

Part I - Government

Chief of Naval Research
Department of the Navy
Arlington, Virginia 22217
Attn: Code 474 (2)

471
222

Director
ONR Branch Office
495 Summer Street
Boston, Massachusetts 02210

Director
ONR Branch Office
219 S Dearborn Street
Chicago, Illinois 60604

Director
Naval Research Laboratory
Attn: Code 2629 (ONRL)
Washington, D.C. 20390 (6)

U.S. Naval Research Laboratory
Attn: Code 2627
Washington, D.C. 20390

Commanding Officer
ONR Branch Office
207 West 24th Street
New York, N.Y. 10011

Director
ONR Branch Office
1030 E. Green Street
Pasadena, California 91101

Defense Documentation Center
Cameron Station
Alexandria, Virginia 22314 (12)

Army

Commanding Officer
U.S. Army Research Off. Durham
Attn: Mr. J. J. Murray
CRD-AA-IP
Box CM, Duke Station
Durham, North Carolina 27706

Commanding Officer
AMXMR-ATL
Attn: Mr. E. Shea
U.S. Army Materials Res. Agency
Watertown, Massachusetts 02172

Watervliet Arsenal
MAGGS Research Center
Watervliet, New York 12189
Attn: Director of Research

Redstone Scientific Info. Center
Chief, Document Section
U.S. Army Missile Command
Redstone Arsenal, Alabama 35809

Army R & D Center
Fort Belvoir, Virginia 22060

Navy

Commanding Officer & Director
Naval Ship Res. & Dev. Center
Bethesda, Maryland 20034
Attn: Code 042 (Tech. Lib. Br.)
17 (Struc. Mech. Lab.)

172
172
174
177
1800(Appl. Math. Lab.)
5412S (Dr. W.D. Sette)
19 (Dr. M.M. Sevik)
1901 (Dr. M. Strassberg)
1945
196 (Dr. D. Feit)
1962

Naval Weapons Laboratory
Dahlgren, Virginia 22448

Naval Research Laboratory
Washington, D.C. 20375

Attn: Code 8400
8410
8430
8440
6300
6390
6380

Undersea Explosion Res. Div.
Naval Ship R&D Center
Norfolk Naval Shipyard
Portsmouth, Virginia 23709
Attn: Dr. E. Palmer
Code 780

Naval Ship Res. & Dev. Center
Annapolis Division
Annapolis, Maryland 21402

Attn: Code 2740 - Dr. Y. F. Wang
28 - Mr. R.J. Wolfe
281 - Mr. Niederberger
2814 - Dr. H. Vanderveldt

Technical Library
Naval Underwater Weapons Center
Pasadean Annex
3203 E. Foothill Blvd.
Pasadena, California 91107

U.S. Naval Weapons Center
China Lake, California 93557
Attn: Code 4062 - Mr. W. Werback
4520 - Mr. Ken Bischel

Commanding Officer
U.S. Naval Civil Engr. Lab.
Code L31
Port Hueneme, California 93041

Technical Director
U.S. Naval Ordnance Lab.
White Oak
Silver Spring, Maryland 20910

Technical Director
Naval Undersea R&D Center
San Diego, California 92132

Supervisor of Shipbuilding
U.S. Navy
Newport News, Virginia 23607

Technical Director
Mare Island Naval Shipyard
Vallejo, California 94592

U.S. Navy Underwater Sound Ref.
Lab.

Office of Naval Research
P.O. Box 8337
Orlando, Florida 32806

Chief of Naval Operations
Dept. of the Navy
Washington, D.C. 20350
Attn: Code Op07T

Strategic Systems Project Off.
Department of the Navy
Washington, D.C. 20390
Attn: NSP- 001 Chief Scientist

Deep Submergence Systems
Naval Ship Systems Command
Code 39522
Department of the Navy
Washington, D.C. 203 60

Engineering Dept.
U.S. Naval Academy
Annapolis, Maryland 21402

Naval Air Systems Command
Dept. of the Navy
Washington, D.C. 20360
Attn: NAVAIR 5302 Aero & Struc.
5308 Struc.
52031F Materials
604 Tech. Lib.
320B Struc.

Director, Aero Mechanics
Naval Air Development Center
Johnsville
Warminster, Pennsylvania 18974

Technical Director
U.S. naval Undersea R&D Center
San Diego, California 92132

Engineering Department
U.S. Naval Academy
Annapolis, Maryland 21402

Naval Facilities Engineering Command
Dept. of the Navy
Washington, D.C. 20360
Attn: NAVFAC 03 Res. & Dev.
04 Res. & Dev.
14114 Tech. Lib.

Naval Sea Systems Command
Dept. of the Navy
Washington, D.C. 20360
Attn: NAVSHIP 03 Res. & Tech.
031 Ch. Scientist R&D
03412 Hydromechanics
037 Ship Silencing Div.
035 Weapons Dynamics

Navy cont.

Naval Ship Engineering Center
Prince George's Plaza
Hyattsville, Maryland 20782
Attn: NAVSEC 6100 Ship Sys Engr &
Des Dep
6102C Computer-Aided
Ship Des
6105G
6110 Ship Concept Des
6120 Hull Div.
6120D Hull Div.
6128 Surface Ship
Struct.
6129 Submarine Struct.

Air Force

Commander WADD
Wright-Patterson Air Force Base
Dayton, Ohio 45433
Attn: Code WWRMDD
AFFDL (FDSD)
Structures Division
AFLC (MCEEA)

Chief, Applied Mechanics Group
U.S. Air Force Inst. of Tech.
Wright-Patterson Air Force Base
Dayton, Ohio 45433

Chief, Civil Engineering Branch
WLRC, Research Division
Air Force Weapons Laboratory
Kirtland AFB, New Mexico 87117

Air Force Office of Scientific
Research
1400 Wilson Blvd.
Arlington, Virginia 22209
Attn: Mechanics Div.

NASA

Structures Research Division
National Aeronautics & Space Admin.
Langley Research Center
Langley Station
Hampton, Virginia 23365

National Aeronautic & Space Admin.
Associate Administrator for Ad-
vanced Research & Technology
Washington, D.C. 02546

Scientific & Tech. Info. Facility
NASA Representative (S-AK/DL)
P.O. Box 5700
Bethesda, Maryland 20014

Other Government Activities

Commandant
Chief, Testing & Development Div.
U.S. Coast Guard
1300 E. Street, N.W.
Washington, D.C. 20226

Technical Director
Marine Corps Dev & Educ. Command
Quantico, Virginia 22134

Director
National Bureau of Standards
Washington, D.C. 20234
Attn: Mr. B.L. Wilson, EN 219

Dr. M. Gaus
National Science Foundation
Engineering Division
Washington, D.C. 20550

Science & Tech. Division
Library of Congress
Washington, D.C. 20540

Director
Defense Nuclear Agency
Washington, D.C. 20305
Attn: SPSS

Commander Field Command
Defense Nuclear Agency
Sandia Base
Albuquerque, New Mexico 87115

Director Defense Research & Engr
Technical Library
Room 3C-128
The Pentagon
Washington, D.C. 20301

Chief, Airframe & Equipment Branch
FS-120
Office of Flight Standards
Federal Aviation Agency
Washington, D.C. 20553

Chief, Research and Development
Maritime Administration
Washington, D.C. 20235

Deputy Chief, Office of Ship Constr.
Maritime Administration
Washington, D.C. 20235
Attn: Mr. U.L. Russo

Atomic Energy Commission
Div. of Reactor Devel. & Tech.
Germantown, Maryland 20767

Ship Hull Research Committee
National Research Council
National Academy of Sciences
2101 Constitution Avenue
Washington, D.C. 20418
Attn: Mr. A.R. Lytle

Part 2 - Contractors and Other
Technical Collaborators

Universities

Dr. J. Tinsley Oden
University of Texas at Austin
345 Eng. Science Bldg.
Austin, Texas 78712

Prof. Julius Miklowitz
California Institute of Technology
Div. of Engineering & Applied Sci.
Pasadena, California 91109

Dr. Harold Liebowitz, Dean
School of Engr. & Applied Science
George Washington University
725 - 23rd St., N.W.
Washington, D.C. 20006

Prof. Eli Sternberg
California Institute of Technology
Div. of Engr. & Applied Sciences
Pasadena, California 91109

Prof. Paul M. Naghdi
University of California
Div. of Applied Mechanics
Etcheverry Hall
Berkeley, California 94720

Professor P.S. Symonds
Brown University
Division of Engineering
Providence, R.I. 02912

Prof. A.J. Durelli
The Catholic University of America
Civil/Mechanical Engineering
Washington, D.C. 20017

Prof. R.B. Testa
Columbia University
Dept. of Civil Engineering
S.W. Mudd Bldg.
New York, New York 10027

Prof. H.H. Bleich
Columbia University
Dept. of Civil Engineering
Amsterdam & 120th St.
New York, New York 10027

Prof. F.L. DiMaggio
Columbia University
Dept. of Civil Engineering
616 Mudd Building
New York, New York 10027

Prof. A.M. Freudenthal
George Washington University
School of Engineering & Applied
Science
Washington, D.C. 20006

D.C. Evans
University of Utah
Computer Science Division
Salt Lake City, Utah 84112

Prof. Norman Jones
Massachusetts Inst. of Technology
Dept. of Naval Architecture &
Marine Engrng
Cambridge, Massachusetts 02139

Professor Albert I. King
Biomechanics Research Center
Wayne State University
Detroit, Michigan 48202

Dr. V.R. Hodgson
Wayne State University
School of Medicine
Detroit, Michigan 48202

Universities cont.

Dean B.A. Boley
Northwestern University
Technological Institute
2145 Sheridan Road
Evanston, Illinois 60201

Prof. P.G. Hodge, Jr.
University of Minnesota
Dept. of Aerospace Engng & Mech.
Minneapolis, Minnesota 55455

Dr. D.C. Drucker
University of Illinois
Dean of Engineering
Urbana, Illinois 61801

Prof. N.M. Newmark
University of Illinois
Dept. of Civil Engineering
Urbana, Illinois 61801

Prof. E. Reissner
University of California, San Diego
Dept. of Applied Mechanics
La Jolla, California 92037

Prof. William A. Nash
University of Massachusetts
Dept. of Mechanics & Aerospace Eng.
Amherst, Massachusetts 01002

Library (Code 0384)
U.S. Naval Postgraduate School
Monterey, California 93940

Prof. Arnold Allentuch
Newark College of Engineering
Dept. of Mechanical Engineering
323 High Street
Newark, New Jersey 07102

Dr. George Herrmann
Stanford University
Dept. of Applied Mechanics
Stanford, California 94305

Prof. J.D. Achenbach
Northwestern University
Dept. of Civil Engineering
Evanston, Illinois 60201

Director, Applied Research Lab.
Pennsylvania State University
P.O. Box 30
State College, Pennsylvania 16801

Prof. Eugen J. Skudrzyk
Pennsylvania State University
Applied Research Laboratory
Dept. of Physics - P.O. Box 30
State College, Pennsylvania 16801

Prof. J. Kempner
Polytechnic Institute of Brooklyn
Dept. of Aero. Engrg & Applied Mech.
333 Jay Street
Brooklyn, N.Y. 11201

Prof. J. Klosner
Polytechnic Institute of Brooklyn
Dept. of Aerospace & Appl. Mech.
333 Jay Street
Brooklyn, N.Y. 11201

Prof. R.A. Schapery
Texas A&M University
Dept. of Civil Engineering
College Station, Texas 77840

Prof. W.D. Pilkey
University of Virginia
Dept. of Aerospace Engineering
Charlottesville, Virginia 22903

Dr. H.G. Schaeffer
University of Maryland
Aerospace Engineering Dept.
College Park, Maryland 20742

Prof. K.D. Willmert
Clarkson College of Technology
Dept. of Mechanical Engineering
Potsdam, N.Y. 13676

Dr. J.A. Stricklin
Texas A&M University
Aerospace Engineering Dept.
College Station, Texas 77843

Dr. L.A. Schmit
University of California, LA
School of Engineering & Applied Sci.
Los Angeles, California 90024

Dr. H.A. Kamel
The University of Arizona
Aerospace & Mech. Engineering Dept.
Tucson, Arizona 85721

Dr. B.S. Berger
University of Maryland
Dept. of Mechanical Engineering
College Park, Maryland 20742

Prof. G.R. Irwin
Dept. of Mechanical Engng.
University of Maryland
College Park, Maryland 20742

Dr. S.J. Fenves
Carnegie-Mellon University
Dept. of Civil Engineering
Schenley Park
Pittsburgh, Pennsylvania 15213

Dr. Ronald L. Huston
Dept. of Engineering Analysis
Mail Box 112
University of Cincinnati
Cincinnati, Ohio 45221

Prof. George Sih
Dept. of Mechanics
Lehigh University
Bethlehem, Pennsylvania 18015

Prof. A.S. Kobayashi
University of Washington
Dept. of Mechanical Engineering
Seattle, Washington 98105

Librarian
Webb Institute of Naval Architecture
Crescent Beach Road, Glen Cove
Long Island, New York 11542

Prof. Daniel Frederick
Virginia Polytechnic Institute
Dept. of Engineering Mechanics
Blacksburg, Virginia 24061

Prof. A.C. Eringen
Dept. of Aerospace & Mech. Sciences
Princeton University
Princeton, New Jersey 08540

Dr. S.L. Koh
School of Aero., Astro. & Eng. Sc.
Purdue University
Lafayette, Indiana 47907

Prof. E.H. Lee
Div. of Engrg. Mechanics
Stanford University
Stanford, California 94305

Prof. R.D. Mindlin
Dept. of Civil Engrg
Columbia University
S.W. Mudd Building
New York, N.Y. 10027

Prof. S.B. Dong
University of California
Dept. of Mechanics
Los Angeles, California 90024

Prof. Burt Paul
University of Pennsylvania
Towne School of Civil & Mech Engr
Rm. 113 - Towne Building
220 S. 33rd Street
Philadelphia, Pennsylvania 19104

Prof. J.W. Liu
Dept. of Chemical Engr. & Metal.
Syracuse University
Syracuse, N.Y. 13210

Prof. S. Bodner
Technion R&D Foundation
Haifa, Israel

Prof. R.J.H. Bollard
Chairman, Aeronautical Engr. Dept.
207 Guggenheim Hall
University of Washington
Seattle, Washington 98105

Prof. G.S. Heller
Division of Engineering
Brown University
Providence, Rhode Island 02912

Prof. Werner Goldsmith
Dept. of Mechanical Engineering
Div. of Applied Mechanics
University of California
Berkeley, California 94720

Prof. J.R. Rice
Division of Engineering
Brown University
Providence, R.I. 02912

Prof. R.S. Rivlin
Center for the Application of
Mathematics
Lehigh University
Bethlehem, Pennsylvania 18015

Libray (code 0384)
U.S. Naval Postgraduate School
Monterey, California 93940

Dr. Francis Cozzarelli
Div. of Interdisciplinary
Studies & Research
School of Engineering
State University of New York
Buffalo, N.Y. 14214

Industry and Research Institutes

Library Services Dept.
Report Section Bldg. 14-14
Argonne National Laboratory
9700 S. Cass Avenue
Argonne, Illinois 60440

Dr. M.C. Junger
Cambridge Acoustical Associates
129 Mount Auburn St.
Cambridge, Massachusetts 02138

Dr. L.H. Chen
General Dynamics Corporation
Electric Boat Division
Groton, Connecticut 06340

Dr. J.E. Greenspon
J.G. Engineering Research Assoc.
3831 Menlo Drive
Baltimore, Maryland 21215

Dr. S. Batdorf
The Aerospace Corp.
P.O. Box 92957
Los Angeles, California 90009

Dr. K.C. Park
Lockheed Palo Alto Research Lab.
Dept. 5233, Bldg. 205
3251 Hanover St.
Palo Alto, CA 94304

Library
Newport News Shipbuilding & Dry
Dock Company
Newport News, Virginia 23607

Dr. W.F. Bozich
McDonnell Douglas Corporation
5301 Bolsa Avenue
Huntington Beach, CA 92647

Dr. H.N. Abramson
Southwest Research Institute
Technical Vice President
Mechanical Sciences
P.O. Drawer 28510
San Antonio, Texas 78284

Dr. R.C. DeHart
Southwest Research Institute
Dept. of Structural Research
P.O. Drawer 28510
San Antonio, Texas 78284

Dr. M.L. Baron
Weidlinger Associates, Consulting
Engineers
110 East 59th Street
New York, N.Y. 10022

Dr. W.A. Rieseemann
Sandia Laboratories
Sandia Base
Albuquerque, New Mexico 87115

Dr. T.L. Geers
Lockheed Missiles & Space Co.
Palo Alto Research Laboratory
3251 Hanover Street
Palo Alto, California 94304

Dr. J.L. Tocher
Boeing Computer Services, Inc.
P.O. Box 24346
Seattle, Washington 98124

Mr. William Caywood
Code BBE, Applied Physics Laboratory
8621 Georgia Avenue
Silver Spring, Maryland 20034

Mr. P.C. Durup
Lockheed-California Company
Aeromechanics Dept., 74-43
Burbank, California 91503

Assistant Chief for Technology
Office of Naval Research, Code 200
Arlington, Virginia 22217

UNCLASSIFIED

SECURITY CLASSIFICATION OF THIS PAGE (When Data Entered)

REPORT DOCUMENTATION PAGE		READ INSTRUCTIONS BEFORE COMPLETING FORM
1. REPORT NUMBER (14) 41	2. GOVT ACCESSION NO.	3. RECIPIENT'S CATALOG NUMBER
(6) 4. TITLE (and Subtitle) New Optical Method to Determine Vibration-Induced Strains with Variable Sensitivity After Recording	5. TYPE OF REPORT & PERIOD COVERED	
	6. PERFORMING ORG. REPORT NUMBER 38479 <i>Qu. Proj 70.</i>	
(10) 7. AUTHOR(s) Y. Y. Hung, J. D. Hovanesian and A. J. Durelli	8. CONTRACT OR GRANT NUMBER(s) N-00014-76-C-0487	
	10. PROGRAM ELEMENT, PROJECT, TASK AREA & WORK UNIT NUMBERS	
9. PERFORMING ORGANIZATION NAME AND ADDRESS Oakland University Rochester, MI 48063		12. REPORT DATE (11) November 1976
11. CONTROLLING OFFICE NAME AND ADDRESS Office of Naval Research Department of the Navy Washington, D.C. 20025		13. NUMBER OF PAGES 31
14. MONITORING AGENCY NAME & ADDRESS (if different from Controlling Office)		15. SECURITY CLASS. (of this report) (12) 26p.1
16. DISTRIBUTION STATEMENT (of this Report) Distribution of this report is unlimited		15a. DECLASSIFICATION/DOWNGRADING SCHEDULE
(15) N00014-76-C-0487 ✓ NSF-ENG-76-08751		
17. DISTRIBUTION STATEMENT (of the abstract entered in Block 20, if different from Report) #		
18. SUPPLEMENTARY NOTES		
19. KEY WORDS (Continue on reverse side if necessary and identify by block number) Vibration Plates Speckle interferometry		
20. ABSTRACT (Continue on reverse side if necessary and identify by block number) A steady-state vibrating object is illuminated with coherent light and its image is slightly misfocused in the film plane of a camera. The resulting processed film is called a "time-integrated specklegram. When the specklegram is Fourier filtered, it exhibits fringes depicting derivatives of the vibrational amplitude. The direction of the spatial derivative, as well as the fringe sensitivity may be easily and continuously varied during the Fourier filtering process. Besides the above mentioned advantages, this		

405252

Y/B

SECURITY CLASSIFICATION OF THIS PAGE(When Data Entered)

new method is also much less demanding than holographic interferometry with respect to vibration isolation, optical set-up time, illuminating source coherence, required film resolution, etc.

Unclassified

SECURITY CLASSIFICATION OF THIS PAGE(When Data Entered)